Research Article | Vol. 25, No. 12 | 12 Jun 2017 | OPTICS EXPRESS 13897
Optics EXPRESS

Surface enhanced nonlinear Cherenkov radiation in one-dimensional nonlinear photonic crystal

XIAOHUI ZHAO,[1,2] YUANLIN ZHENG,[1,2] NING AN,[3] XUEWEI DENG,[4] HUAIJIN REN,[5,6] AND XIANFENG CHEN[1,2,*]

[1]*State Key Laboratory of Advanced Optical Communication Systems and Networks, Department of Physics and Astronomy, Shanghai Jiao Tong University, 800 Dongchuan Road, Shanghai 200240, China*
[2]*Key Laboratory for Laser plasmas (Ministry of Education), Collaborative Innovation Center of IFSA (CICIFSA), Shanghai Jiao Tong University, 800 Dongchuan Road, Shanghai 200240, China*
[3]*Shanghai Institute of Laser Plasma, China Academy of Engineering Physics, Shanghai, 201800 China*
[4]*Laser Fusion Research Center, China Academy of Engineering Physics, Mianyang, Sichuan 621900, China*
[5]*Institute of Applied Electronics, China Academy of Engineering Physics, Mianyang, Sichuan 621900, China*
[6]*renhuaijin@caep.cn*
[*]*xfchen@sjtu.edu.cn*

Abstract: We study the configuration of efficient nonlinear Cherenkov radiation generated at the inner surface of a one-dimensional nonlinear photonic crystal, which utilizes the combination of both quasi-phase matching and total internal reflection by the crystal surface. Multidirectional nonlinear Cherenkov radiation assisted by different orders of reciprocal vectors is demonstrated experimentally. At specific angles, by associating with quasi-phase matching, the incident fundamental wave and total internal reflection wave format completely the phase-matching scheme, leading to great enhancement of harmonic wave intensity.

OCIS codes: (190.0190) Nonlinear optics; (190.4350) Nonlinear optics at surfaces; (190.2620) Harmonic generation and mixing.

References and links

1. A. Zembrod, H. Puell, and J. Giordmaine, "Surface radiation from non-linear optical polarisation," Opt. Quant. Electron. **1**, 64–66 (1969).
2. Y. Zhang, Z. Gao, Z. Qi, S. Zhu, and N. Ming, "Nonlinear Čerenkov radiation in nonlinear photonic crystal waveguides," Phys. Rev. Lett. **100**, 163904 (2008).
3. P. Tien, R. Ulrich, and R. Martin, "Optical second harmonic generation in form of coherent Cerenkov radiation from a thin-film waveguide," Appl. Phys. Lett. **17**, 447–450 (1970).
4. M. J. Li, M. De Micheli, Q. He, and D. Ostrowsky, "Cerenkov configuration second harmonic generation in proton-exchanged lithium niobate guides," IEEE J. Quantum Electron. **26**, 1384–1393 (1990).
5. H. Huang, C. Huang, C. Zhang, D. Zhu, X. Hong, J. Lu, J. Jiang, Q. Wang, and Y. Zhu, "Second-harmonic generation in a periodically poled congruent $LiTao_3$ sample with phase-tuned nonlinear Cherenkov radiation," Appl. Phys. Lett. **100**, 022905 (2012).
6. L. Mateos, P. Molina, J. Galisteo, C. López, L. E. Bausá, and M. O. Ramírez, "Simultaneous generation of second to fifth harmonic conical beams in a two dimensional nonlinear photonic crystal," Opt. Express **20**, 29940–29948 (2012).
7. C. Chen, J. Lu, Y. Liu, X. Hu, L. Zhao, Y. Zhang, G. Zhao, Y. Yuan, and S. Zhu, "Cerenkov third-harmonic generation via cascaded $\chi^{(2)}$ processes in a periodic-poled $LiTao_3$ waveguide," Opt. Lett. **36**, 1227–1229 (2011).
8. Y. Sheng, W. Wang, R. Shiloh, V. Roppo, Y. Kong, A. Arie, and W. Krolikowski, "Čerenkov third-harmonic generation in $\chi^{(2)}$ nonlinear photonic crystal," Appl. Phys. Lett. **98**, 241114 (2011).
9. N. An, H. Ren, Y. Zheng, X. Deng, and X. Chen, "Cherenkov high-order harmonic generation by multistep cascading in $\chi^{(2)}$ nonlinear photonic crystal," Appl. Phys. Lett. **100**, 221103 (2012).
10. P. M. Paul, E. S. Toma, P. Breger, G. Mullot, F. Auge, P. Balcou, H. G. Muller, and P. Agostini, "Observation of a train of attosecond pulses from high harmonic generation," Science **292**, 1689–1692 (2001).
11. X. Deng, H. Ren, H. Lao, and X. Chen, "Research on Cherenkov second-harmonic generation in periodically poled lithium niobate by femtosecond pulses," J. Opt. Soc. Am. B **27**, 1475–1480 (2010).

#292756 https://doi.org/10.1364/OE.25.013897
Journal © 2017 Received 13 Apr 2017; revised 24 May 2017; accepted 1 Jun 2017; published 9 Jun 2017

Optics EXPRESS

12. Y. Sheng, A. Best, H.-J. Butt, W. Krolikowski, A. Arie, and K. Koynov, "Three-dimensional ferroelectric domain visualization by Čerenkov-type second harmonic generation," Opt. Express **18**, 16539–16545 (2010).
13. Y. Zhang, J. Wen, S. N. Zhu, and M. Xiao, "Nonlinear Talbot Effect," Phys. Rev. Lett. **104**, 183901 (2010).
14. Y. Sheng, V. Roppo, K. Kalinowski, and W. Krolikowski, "Role of a localized modulation of $\chi^{(2)}$ in Čerenkov second-harmonic generation in nonlinear bulk medium," Opt. Lett. **37**, 3864–3866 (2012).
15. X. Zhao, Y. Zheng, H. Ren, N. An, X. Deng, and X. Chen, "Nonlinear Cherenkov radiation at the interface of two different nonlinear media," Opt. Express **24**, 12825–12830 (2016).
16. H. Ren, X. Deng, Y. Zheng, N. An, and X. Chen, "Surface phase-matched harmonic enhancement in a bulk anomalous dispersion medium," Appl. Phys. Lett. **103**, 021110 (2013).
17. H. Ren, X. Deng, Y. Zheng, N. An, and X. Chen, "Enhanced nonlinear Cherenkov radiation on the crystal boundary," Opt. Lett. **38**, 1993–1995 (2013).
18. V. Roppo, K. Kalinowski, W. Krolikowski, K. Wieslaw, C. Cojocaru, and J. Trull, "Unified approach to Čerenkov second harmonic generation," Opt. Express **21**, 25715–25726 (2013).
19. O. Gayer, Z. Sacks, E. Galun, and A. Arie, "Temperature and wavelength dependent refractive index equations for MgO-doped congruent and stoichiometric $LiNbO_3$," Appl. Phys. B **91**, 343–348 (2008).
20. H. Ren, X. Deng, Y. Zheng, N. An, and X. Chen, "Nonlinear Cherenkov radiation in an anomalous dispersive medium," Phys. Rev. Lett. **108**, 223901 (2012).
21. Y. Sheng, Q. Kong, V. Roppo, K. Kalinowski, Q. Wang, C. Cojocaru, and W. Krolikowski, "Theoretical study of Čerenkov-type second-harmonic generation in periodically poled ferroelectric crystals," J. Opt. Soc. Am. B **29**, 312–318 (2012).

1. Introduction

When the phase velocity of nonlinear polarization wave (v_p) exceeds that of its harmonic wave (v') in a nonlinear medium, coherent harmonic wave emits, known as nonlinear Cherenkov radiation (NCR) [1]. The Cherenkov angle is defined as $\theta = \arccos(v_p/v')$, which implies the automatically longitudinal phase-matching condition between the fundamental and the radiated harmonic wave. In $\chi^{(2)}$ photonic crystals [2], waveguides [3, 4] and other micro-structures, Cherenkov radiation could demonstrate possibilities of a wide variety of phase-matching types and diverse patterns of spatial distribution, such as, the phase-tuned Cherenkov-type interaction in two dimensional nonlinear photonic crystals [5], the quasi-phase matching (QPM) associated NCR generated in waveguides or nonlinear $\chi^{(2)}$ crystals [6], domain wall enhanced high-order NCR [7–9]. Such modulation mechanism has greatly expanded the NCR radiation characteristics, providing potential applications for short wavelength lasers [10], broadband frequency doubling [11] and optical imaging [12, 13].

In addition, the efficiency of NCR is dramatically affected by the abrupt change of the second-order nonlinearity $\chi^{(2)}$, which contains not only the -1 to 1 $\chi^{(2)}$ modulation corresponding to the domain wall but also the 0 to 1 modulation corresponding to the crystal surface [14, 15]. By using sum-frequency polarization wave generated by incident and internal total reflected waves [16], previous studies have achieved enhanced NCR on the crystal surface [17, 18]. Such NCR can provide good light quality and relatively high efficiency, which allows for further practical applications, such as nondestructive diagnostics, harmonic conversion and ultrashort pulse characterization.

In this work, we study the behavior of NCR generated at the crystal surface which can be modulated by the $\chi^{(2)}$ microstructure at the surface. Using the coupled wave equation, we also demonstrate the effect of reciprocal vectors of photonic crystals to the radiation angles of NCR. When the internal reflection inside the crystal boundary is utilized, the sum-frequency polarization of the incidences assisted with different orders of reciprocal vectors can emit multiple NCRs which exhibits $\chi^{(2)}$ spatially modulated pattern. Particularly, at specific incident angles, one can achieve degenerated NCR which leads to remarkable enhancement on the intensity.

2. Phenomenon and analysis

For simplicity, here we choose a one-dimensional (1D) periodically poled $LiNbO_3$ crystal (PPLN) as the sample. It provides uniform collinear reciprocal vectors along x-axis and the pol-

Optics EXPRESS

ing period is $\Lambda = 6.92\ \mu$m. The sample was put on a rotation stage which can be adjusted in the y-z plane, as shown in Fig. 1(a). According to the calculation of the Sellmeier equation [19], the refractive index of ordinary-polarized fundamental wave is larger than that of the extraordinary-polarized second harmonic (SH) wave when the wavelength of pump is longer than 1023 nm. Consequently, it provides an anomalous-dispersion-like medium by utilizing type I (oo-e) second harmonic (SH) phase-matching scheme [20]. The light source in the experiment was an optical parametric amplifier (TOPAS, Coherent Inc.) producing 80 femtosecond pulses (1000 Hz rep. rate) at the variable wavelengths from 280 nm to 2600 nm. A quarter-wave plate and a Glan-Taylor prism was used to adjust the polarization. Then the laser beam was loosely focused to a beam width of 50 μm and was incident into the y-z plane of the sample. A screen was located 10 cm behind the sample to receive the emitted patterns. The operating temperature was 20°C.

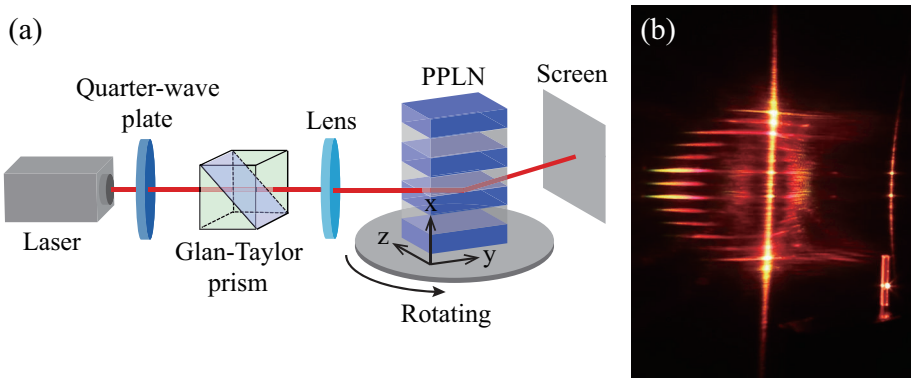

Fig. 1. (a) The diagram of experimental setup; (b) Multiple nonlinear Cherenkov diffraction pattern recorded in the experiment.

When the ordinary-polarized fundamental wave (FW) with a wavelength of 1250 nm was injected into the sample along y-axis, NCR didn't emerge owing to the phase-matching condition being not satisfied in such anomalous dispersion. When the sample was pivoted with x-axis, the fundamental beam would be reflected on the x-y plane while the incident angle exceed the requirement of total reflection inside the sample. By adjusting the incident angle of FW, and combining the total reflection wave and reciprocal vectors, the sum-frequency polarization along the crystal surface would give birth to NCR. The far-filed image of SH wave on the screen is shown in Fig. 1(b). The straight line in the middle is the nonlinear Raman-Nath diffraction generated from the sum-frequency of incident FW and total reflection, while the right arc line belongs to the conical scattering SH wave. The fascinating phenomenon occurred at the left of the sum-frequency Raman-Nath diffraction, where multiple Cherenkov diffraction patterns with transverse angular dispersion located on an arc array. Distinguished from the phenomenon in the bulk material [17, 18], the pattern exhibits periodically spatial distribution, which denotes the reciprocal-involved NCR by total reflection on the PPLN surface.

To analyze the distribution of SH, the coupled wave equation under paraxial and small-signal approximation was solved by using the Fourier transform method. The intensity of SH I_2 is expressed as [15, 21]:

$$I_2(k_x, k_z) = \left[\frac{k_2}{2n_2^2}\chi^{(2)}\right]^2 I_1^2 L^2 \mathrm{sinc}^2\left[\left(k_2 - 2k_1\cos\alpha - \frac{k_x^2 + k_z^2}{2k_2}\right)\frac{L}{2}\right]|F(k_x)|^2|G(k_z)|^2, \quad (1)$$

where n_2 is the refractive index of SH, I_1 denotes the complex amplitude of the Gaussian FW with width a, L is the interaction distance of the nonlinear process, α is the incident angle of

Optics EXPRESS

FW along y axis, k_1 and k_2 are wave vectors of the FW and SH, respectively. In the expression, $2k_1\cos\alpha = |\vec{k_1} + \vec{k_1'}|$, where $\vec{k_1'}$ is the wave vector of the reflected FW. k_x and k_z are the components of k_2 in x-axis and z-axis. $F(k_x) = \sqrt{\frac{\pi}{2}}a\sum_n g_n e^{-a^2(nG_0-k_x)^2/8}$ and $G(k_z) = \sqrt{\frac{\pi}{8}}ae^{-a^2k_z^2/8} + i\frac{\sqrt{2}}{2}aD\left(\frac{ak_z}{8}\right)$ are the Fourier transformations of the $\chi^{(2)}$ modulated structures, which are introduced by periodically reversed domains and the crystal boundary, respectively. Here g_n are the Fourier coefficients which can be expressed as:

$$g_n = \{ \quad 2\sin(n\pi d)/(n\pi) n \neq 0 \; 2d - 1 n = 0,$$

where n are integers. $G_0 = 2\pi/\Lambda$ denotes the 0-order reciprocal vector of the sample, d is the duty ratio of domain reversal. $D\left(\frac{ak_z}{8}\right)$ denotes the Dawson function. The intensity of SH is positively correlated with the beam width.

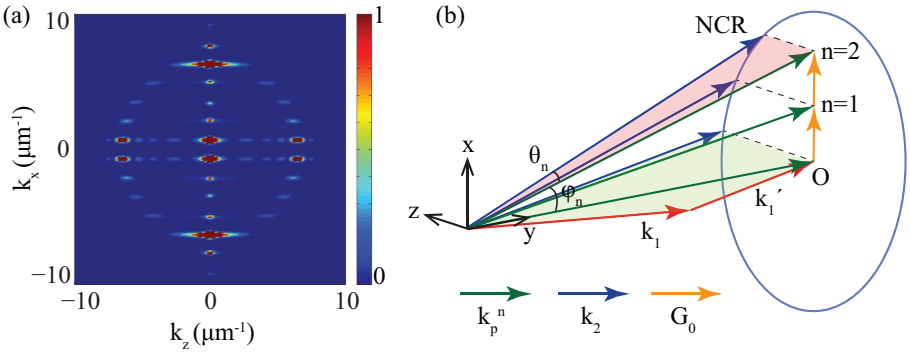

Fig. 2. (a) Simulation result of SH distribution with a FW incident angle of $\alpha = 20°$; (b) Phase-matching geometry.

The simulation result of SH distribution is shown in Fig. 2(a) under the same condition with the experiment in Fig. 1(b), and the FW incident angle is $\alpha = 20°$. Multiple NCRs was distributed on a circle. The SH pattern has the similar pattern with Fig. 1(b). But the right half was total reflected in experiment. Actually, the incident angle has an error with that in the experiment. So the highest order in experiment is 6 and in the simulation result is 5. The 0-order nonlinear Cherenkov radiation was missing. Because the duty ratio of domain reversal in the simulation is $\frac{1}{2}$, and the Fourier coefficient of 0-order reciprocal vector $g_0 = 0$. From Eq. (1), we can find that, when $k_z = 0$, the SH intensity I_2 gathers in the direction defined by $k_x = nG_0$, which represents the nonlinear Raman-Nath diffraction. When $k_z \neq 0$, SH will radiate at angles satisfing the conditions $k_x = nG_0$ and $k_2 - 2k_1\cos\alpha - \frac{k_x^2+k_z^2}{2k_2} = 0$. Under the paraxial approximation, the solution of the latter is $k_x^2 + k_z^2 + (2k_1\cos\alpha)^2 = k_2^2$, which is exactly the longitudinal phase-matching condition of NCR. The corresponding phase-matching geometry is shown in Fig. 2(b). The emission of 0-order NCR in the experimental pattern is in accordance with the situation in bulk material [17]. For high-order NCR, one should take reciprocal vectors into consideration, which is associated with Fourier components of the $\chi^{(2)}$ modulation in terms of QPM along the x-axis. The nonlinear sum-frequency polarization wave along the reflection interface (x-y plane) associating with the reciprocal vectors along the y-axis simulates an effective polarization wave which could emit high order Cherenkov radiation. The wave vector of nonlinear polarization wave of n-order NCR has the form: $\vec{k_p^n} = |\vec{k_1} + \vec{k_1'} + n\vec{G_0}|$. And the radiation angle of n-order NCR along x axis is deduced:

$$\varphi_n = \arctan\frac{nG_0}{2k_1\cos\alpha}, \tag{2}$$

Optics EXPRESS

and along z axis:

$$\theta_n = \arccos\frac{\overline{(nG_0)^2 + (2k_1\cos\alpha)^2}}{k_2}. \tag{3}$$

3. Experimental results and discussion

To experimentally demonstrate the calculated relationship of n-order NCR angle, we investigated the external angles of different order Cherenkov radiations varying with the incident wavelength, with fixed the FW external incident angle of $i = 30°$. The distance of the FW and SH on the screen were measured. The radiation angles were calculated, according to the geometrical relationship. The measurement error of angles was kept within ±0.5°. And with fixed wavelength of FW $\lambda = 1250$ nm, we measured the relationship between the external emergence angles and the external incident angles. The experimental results, demonstrate good agreement with theoretical predications, as shown in Figs. 3(a) and 3(b), respectively. According to the phase-matching condition and the experimental results, we verify that the polarization wave is always confined along the crystal surface.

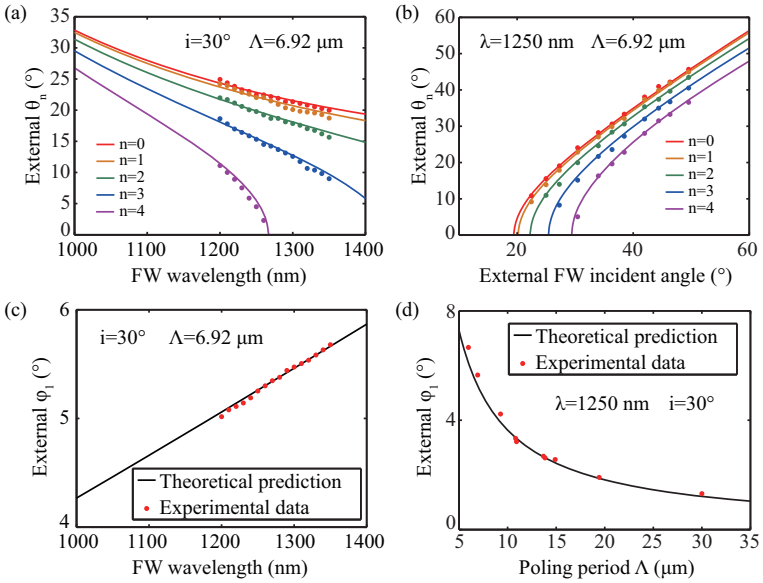

Fig. 3. The external angles along z-axis of different order NCRs versus the incident wavelength of FW (a) and external incident angle (b). The relationship of external angles along x-axis of 1-order NCR varying with the incident wavelength (c) and the poling period of PPLN (d). Theoretical prediction (solid curves) and experimental results (signs) are in well agreement with each other.

Furthermore, we investigated the transverse distribution of the nonlinear diffraction along x-axis. With the external incident angle fixed at 30°, the external angles of the 1-order Cherenkov radiation varied with the incident wavelength [Fig. 3(c)]. When the wavelength of FW was fixed at 1250 nm, we draw the relationship between diffraction angles and the periods by using several samples, as shown in Fig. 3(d). The angular positions of nonlinear Cherenkov radiation patterns varied with the variance of the samples, which imply that the periodical structure are modulated the surface reflecting Cherenkov radiation. The transversely spatial distribution (along x-axis) of nonlinear Cherenkov patterns coincided with nonlinear Raman-Nath diffraction in 1D nonlinear crystal.

Optics EXPRESS

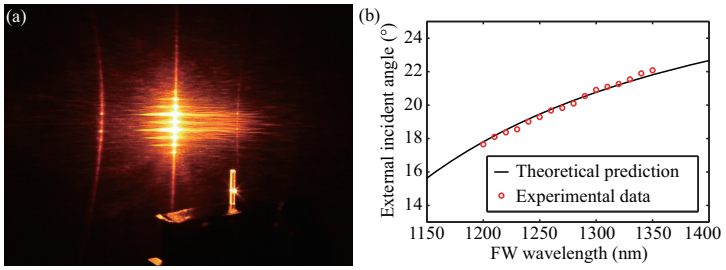

Fig. 4. (a) Recorded pattern of enhanced 0-order NCR. (b) The external FW angles of enhanced 0-order NCR versus the incident wavelength of FW.

In Fig. 3(b), we note that each order of NCR has a cutoff angle. At these incident angles, the emission angle of corresponding order NCR equals to 0. The phase-matching condition can be written as $\vec{k_p^n} = |\vec{k_1} + \vec{k_1'} + n\vec{G_0}| = \vec{k_2}$, where the polarization wave is collinear with the Cherenkov harmonic wave and the phase-mismatch is minimized. Therefore each order of NCR would be greatly enhanced at these specific angles. In experiment, it is clearly that such enhancement occurred at the beginning of the NCR emergence.

We recorded the enhanced 0-order NCR with a FW wavelength of 1250 nm, as shown in Fig. 4(a). The multiple dots along x-axis are the nonlinear Raman-Nath diffractions. The intensity of SH is significantly greater than that in the previous experiment. In Fig. 4(b) we verified the dependence of the incident angle of the enhanced 0-order NCR as a function of the incident wavelength. The incident angle increases proportionally with the incident wavelength, which is consistent with theoretical analysis. So far, we have realized the modulation of both diffraction pattern and the efficiency of Cherenkov diffraction on the PPLN surface, which provide more plentiful radiation patterns compared with NCR on bulk crystal surfaces.

4. Conclusion

In summary, we experimentally demonstrated the $\chi^{(2)}$ modulated nonlinear Cherenkov diffraction on the PPLN surface. The sum-frequency polarization wave generated by incident and reflected waves was confined on the crystal surface and modulated by the periodical $\chi^{(2)}$ structure. The diffraction angle and transverse distribution of the QPM-NCR were investigated experimentally, which shows a good agreement with the theoretical calculation. In addition, with proper incident angles, the multiple diffraction would be greatly enhanced, which features the NCR emergence. It present that more plentiful radiation patterns could be expected in other $\chi^{(2)}$ structures, such as aperiodic, quasi-periodic, random, chirp, two-dimensional and other desirable patterns. Further, making appropriate artificial structures on the crystal surface would allow us to control the behavior of harmonic generation more efficiently.

Funding

National Basic Research Program 973 of China (2011CB808101); National Natural Science Foundation of China (61125503, 61235009, 61205110, 61505189 and 11604318); Innovative Foundation of Laser Fusion Research Center; Presidential Foundation of the China Academy of Engineering Physics (201501023).